

U.S. Department of the Interior

U.S. Geological Survey

Modelling of a magnetic and gravity anomaly profile from the Dragoon Mountains
to Sierra Vista, southeastern Arizona

by

Paul E. Gettings and Mark E. Gettings¹

Open-File Report 96-288

This report is preliminary and has not been reviewed for conformity with U.S. Geological Survey editorial standards or with the North American Stratigraphic Code. Any use of trade, firm, or product names is for descriptive purposes only and does not imply endorsement by the U.S. Government.

¹U.S. Geological Survey, Southwest Field Office, 406 Gould-Simpson Building, University of Arizona, Tucson, Arizona, 85721

Abstract

A total intensity magnetic field anomaly profile acquired with a truck-borne proton precession magnetometer and the corresponding regional complete Bouguer gravity anomaly profile were modelled to obtain a self-consistent and geologically reasonable model which produces good fits to the gravity and magnetic anomaly fields. The profile extends from the west side of the Dragoon Mountains near Middlemarch Canyon southwest to Tombstone, and thence to Sierra Vista, ending at the east gate of the Fort Huachuca Military Reservation in Cochise County, southeastern Arizona. The model predicts that the unconsolidated fill in both the basin northeast and the one southwest of the Tombstone Hills is relatively thin. The model indicates that the total depth of the San Pedro basin in the Sierra Vista-east gate Fort Huachuca part of the profile is about 2950 ft (900m). In the basin northeast of the Tombstone Hills the maximum model depth is about 6600 ft (2000m), but 50% or more of the fill may be Tertiary volcanic rocks. In both basins the model predicts that the unconsolidated fill is only of the order of 30% or less of the total volume of fill. The model implies that there is at least one and probably more bedrock highs in the Sierra Vista area with depths to bedrock of about 700 ft (200m).

Introduction

This work was undertaken as part of a larger project to delineate the geometric form and subsurface geologic structure of the southern San Pedro River basin in southeastern Arizona. In addition to their interest from a general tectonic standpoint, the subbasin distribution and the location of the controlling structures have important implications for mineral resource studies and ground water issues, especially if the basin fill is not too deep. The southern San Pedro River basin basin fill consists of a consolidated, generally conglomeritic lower unit which is commonly tilted, overlain by more gently dipping, generally unconsolidated alluvium (Hayes and Raup, 1968; Drewes, 1980). The consolidated fill is exposed at the foot of the northern and northeastern Huachuca Mountains and east of the Tombstone Hills but its presence and extent in the subsurface is unknown except where identified in drillholes in the Fort Huachuca and Sierra Vista areas (Brown and others, 1966; U.S. Army Corps of Engineers, 1974). As the unconsolidated fill is usually highly permeable, its thickness is important. The gravity method is often used to estimate basin fill thicknesses, but it is difficult to isolate the gravity effect of the unconsolidated fill from the consolidated fill below using gravimetric methods alone (see, for example, Ellett, 1994). Although the unconsolidated fill is generally less dense than the consolidated fill (see, for example, Tucci and others, 1982), without an independent depth estimate of one of the interfaces, the gravity anomaly alone cannot distinguish between two layers of different densities and one of the average density of the two. Halvorson (1984) and Gettings and Houser (1995) have produced estimates of depth of fill in the southern San Pedro basin but neither of these studies attempted to separate consolidated from unconsolidated fill. The object of the work described here was to test the idea that by using magnetic anomaly data to define the depth to bedrock of the basin, gravity anomaly data could be used to map

the interface between the less dense unconsolidated and the more dense consolidated fill units. Requiring the whole model to fit both the magnetic and gravity anomaly data and be geologically reasonable would then yield a self-consistent model.

A profile which extends from the west side of the Dragoon Mountains near Middlemarch Canyon southwest to Tombstone, across the Tombstone Hills to Charleston, and thence southwest to Sierra Vista and the East Gate of Fort Huachuca was chosen. Because of volcanic rocks intercalated in the consolidated fill northeast of Tombstone, and the variety of terrane crossed, this profile proved to be a good one for evaluating the hypothesis.

Data Acquisition and Processing

Geologic data

A geologic basemap for the study area is shown in Plate 1. It was compiled mainly from the maps of Drewes (1980) and Moore (1993). In compiling the map, pre-San Pedro basin fill was divided into several units. Because there are Tertiary intrusive and extrusive rocks of andesitic to rhyolitic composition, some of which are within the basin fill east of Tombstone Caldera, (Tg, TKp and Tv on Pl. 1), as well as Cretaceous ones (Kgd, Kut and Kbv, Pl. 1), these units as well as the Cretaceous sedimentary units have been broken out from the older rocks. Where known, consolidated fill has also been shown (Tc, Pl.1). In the area of the Tombstone Caldera, the rocks of the caldera event (Kut and Ktg, Pl.1) defined by Moore (1993) have been shown separately from the pre-caldera Cretaceous rocks which are comprised of the Bronco volcanics (Gilluly, 1956) and the sediments of the Bisbee Formation, because there could be a large change in thickness of volcanic rocks as the caldera ring fault is crossed. However, the existence of numerous outcrops of pre-caldera rocks both within and without the caldera (Pl.1) suggests that no thickness of volcanic rocks much greater than that observed is to be expected.

The unit mapped as PzX (Pl. 1) comprises a variety of rocks from Precambrian granite through Paleozoic sedimentary rocks. The rocks of the Bisbee Formation (Kb, Pl. 1) and the Cretaceous sedimentary rocks in the southern Mustang Hills (Ks, Pl.1) are Lower Cretaceous in age (Drewes, 1980) and are overlain in the central study area by the Bronco Volcanics (Kbv, Pl.1) which are dated at 76 Ma and older (Moore, 1993). The rocks of the Tombstone caldera (Kut and Kgd, Pl.1) are only slightly younger at 73-76 Ma (Moore, 1993). The youngest rocks known in the Tombstone caldera area (TKp, Pl.1) are rhyolite dikes and plugs which have yielded 64-67 Ma dates (Moore, 1993). The Tertiary volcanic rocks to the east of Tombstone and along the Babocomari River in the southern Mustang Hills (Tv, Pl.1) are dated at 22-39 Ma (Drewes, 1980) and generally lie on consolidated Tertiary fill (Tc, Pl.1) which varies in age from Oligocene to mid-Miocene. The base of unconsolidated fill (QTal, Pl.1) may be as old as Upper Miocene; one small area of basalt on fill northeast of Tombstone is probably 1-3 Ma in age (Drewes, 1980).

Gravity anomaly surveys have shown that the southern San Pedro River basin in

the Sierra Vista-Tombstone area is composed of two subbasins, one to the west of the Tombstone Hills and the other to the northeast (Halvorson, 1984; M.E. Gettings, written communication, 1995). The basin northeast of the Tombstone Hills has the largest mass deficiency as measured by the gravity anomaly, and the gravity anomaly minimum ("low") is spatially more extensive (M.E. Gettings, written communication, 1995). The San Pedro basin south of the Tombstone Hills is composed of a single large subbasin between the Mule Mountains and the Huachuca Mountains, and is probably a half graben with the range-front fault on the Huachuca Mountains (west) side (Gettings and Houser, 1995).

Some drillhole information is available in the Sierra Vista-Fort Huachuca area. Hole DH1 on Pl. 1 is a water well (Arizona Dept. Water Resources File No. D(21-20)35abb, 35-67747) which penetrated bedrock believed to be granite from 780-975 ft (238-297 m). Hole DH2 (Pl.1) is Test Well #8 on the Fort Huachuca Military Reservation (U.S. Army Corps of Engineers, 1974) which penetrated Bronco volcanics at 1295-1501 ft (395-458 m) and consolidated fill from 632-1295 ft (193-395 m). In both wells the rather shallow depth of unconsolidated fill is notable. Geophysical logs of DH2, including a compensated gamma density log, became available during this study (U.S. Army Corps of Engineers, 1974) and yielded the following mean bulk densities for geophysically defined units: upper fill 0-700 ft depth (0-213 m), 2.11 g/cc; consolidated fill 700-1295 ft depth (213-395 m) 2.39 g/cc; and volcanics 1295-1501 ft depth (395-458 m), 2.50 g/cc. Mean logged porosities for these intervals were: fill 33%; consolidated fill 18%; and volcanics 9%.

Magnetic Anomaly Data

Acquisition of the magnetic field data was completed using a truck-mounted proton-precession magnetometer. The data were recorded with a nominal spacing of five meters along the ground, at a constant height of three meters above the surface. Only the total field was measured. These data were extracted from an archive prepared previously by Gettings, et al. (1995) which contains anomaly values which have been corrected for instrument heading, diurnal drift, and the International Geomagnetic Reference Field. For use in the modeling software (see below), the magnetic profile was required to contain less than 201 datum points. To accommodate this, the processed magnetic data were selectively filtered. This filter took the form of an extraction algorithm that would extract every n th point. The original profile had a total of 6055 datum points. By applying the extraction algorithm twice in succession, first for every third, then for every tenth point, a final profile was created with the required maximum of 200 points. This file was then edited by hand to remove three extraneous points which had been selected. These points were extremely sharp spikes caused by the magnetic field associated with bridges. Each point was determined to be caused by a bridge by examining the original, unfiltered data to determine the width of the peak. If the peak was found to be only a few points wide, meaning only a few meters width, the point spike was considered to be a bridge. Examination of the field notes, which record all observed bridges and other magnetic objects, also determined the cause of the spike. After filtering, the profile was projected to a straight azimuth to allow the use in the

modeling software, which expects a straight profile. As the profile had a sharp turn at the southwest end, the profile was broken apart at that point and projected to two azimuths, N 39 degrees E for the northeast segment and east-west for the approximately 5 km long segment at the southwest end. The resulting two pieces were concatenated after adding an offset to account for the different starting origins. The projected data profile was used as the data for all the modeling. The plan locations of the data points and the projected profile are shown on Plate 1. Plate 2 shows the 6055 point magnetic field anomaly profile plotted as a function of down-line distance (not projected) at a scale of 1:125,000.

The magnetic data have three large data gaps (Pl.2). The first data gap is unexplained, but presumably due to a large culvert or bridge, which causes the magnetometer to lose signal until the field becomes stable again. If the truck continues moving, the magnetometer will often not recover signal for a long distance. The other two data gaps are attributed to bridges. In both cases the magnetometer did not quickly recover, hence the data gap.

Gravity Anomaly Data

Gravity anomaly data were digitized from a 1:125,000 scale complete Bouguer gravity anomaly map (Gettings and Houser, 1995) which covered the entire extent of the truck magnetometer route. After digitizing the gravity anomaly contour values along the truck route, the profile was also projected to the two azimuths in the same manner as the magnetic data. Both profiles were projected to the same origin as well, allowing for simultaneous use of both data sets in the modeling.

Initial Model & Software

The modeling was accomplished through the use of the program **saki**, which allows for both forward calculation and least-squares inversion of magnetic and gravity anomaly data (Webring, 1985; Phillips and others, 1993). The models are based on right prisms of polygonal cross-section, each with its own constant density and magnetic susceptibility.

The initial model was determined by the magnetic signal and the geologic map of the area (Drewes, 1980). The extent of the basin model perpendicular to the profile path was determined from the width of basin fill material on the geologic map. As both basins were found to be very similar in extent northwest-southeast, the same length extent perpendicular to the profile was used for all prisms. By map measurement, the prism length was fixed at 30 km symmetric about the profile. The edges of the prisms were determined by the major gradients and changes in the magnetic signal. The gravity anomaly data played a large part in the determination of the initial model. Initial depth to bedrock for the eastern half of the profile was found by measuring the gravity anomaly of the basin, treating it as an inverted spherical cap (Duska, 1958), and calculating the depth of rock necessary to produce the observed anomaly, assuming a density contrast of -0.4 g/cc . Referring to the geologic map showed where on the profile the truck's route crossed onto exposed bedrock. These points were used to fix the edges of the two basins in the initial

model. Since the modelling began with the magnetic data only, the fill of the basins was omitted and the magnetic basement was extended to a depth of 11 km, making it essentially infinite. This prevents the shape of the bottom of the model having any great effect on the model, allowing concentration on the upper boundary between bedrock and fill.

After establishing an initial model from the gravity anomaly and geologic maps, it was found that a simultaneous fit of both basins was extremely cumbersome. To ease modelling, the profile was split in half over the exposed bedrock at the large data gap present at 22.5 km. This made modeling of the data much simpler and also allowed for a closer fit of each portion than was practical using the entire profile at once.

Modeling Procedure

Modeling was conducted in two stages. First, the magnetic profile was fit using the bedrock and assuming a nonmagnetic basin fill. Once a suitable fit to the magnetic anomaly profile had been achieved, then the (nonmagnetic) fill of the basins was added in and the model fitted to both gravity and magnetic anomalies simultaneously. To provide additional constraints for the modelling, a map of low level aeromagnetic profiles of the area was prepared from the National Uranium Resource Evaluation (NURE) survey data (Texas Instruments Inc., 1979) and is shown in plate 3.

To fit the magnetic data, both the susceptibility and the geometric shapes of the bodies were changed. The modeling software was allowed to invert on both parameters in small groups, so as to constrain the inversion algorithm. Each run of the inversion was checked to insure that no geologically impossible results had been obtained. The fitting of the model to the data was an iterative process, with constant revision of the model to allow for better fits in the face of difficulties in inversion, and further study of the geologic, magnetic, and gravity maps.

After obtaining a suitable fit to the magnetic data, the basin fill was added to the model and the gravity anomaly modelled. Initial attempts were done by having only one density of basin fill and allowing the software to invert on the geometry of the prisms and on the density contrasts. Like the magnetic model fitting, the results of the inversion were checked to insure plausibility in the face of the known data from drill logs and geologic mapping. Density contrasts for the basin fill were estimated to be at an initial value of -0.4 g/cc. It was soon found that a single-layer model of basin fill would not fit the gravity data satisfactorily while simultaneously fitting the magnetic anomaly, so a multi-layer model was designed. To account for changing density with depth, two horizontal layers were incorporated to allow for varying density contrasts. Initial estimates of the contrasts were -0.6 g/cc for the upper fill, and -0.4 g/cc for the lower fill, based on the results of Cordell (1973) and density logs of drillholes in the Fort Huachuca area (U.S. Army Corps of Engineers, 1974) and other basins in southern Arizona (Tucci and others, 1982). By then inverting on the geometry and densities of the fill layers, a satisfactory fit was achieved to

both the gravity and magnetic anomaly profiles.

Although the simple procedure outlined above sufficed for the western half of the profile, fitting the potential field anomaly data of the eastern half was more complex. By studying the geologic map (Drewes, 1980), it was determined that the lower, more dense fill was actually overlain by a layer of volcanic rocks. These volcanics were found to be less dense from the gravity map, and also magnetic and in part reversely polarized from the NURE profiles (see plate 3 overlain on plate 1). By placing a layer of volcanics and dense fill on top of a deeper bedrock, the magnetic fit was maintained and the gravity fit as well. The standard two layer basin fill model of the western half was placed in the eastern basin as well, as it was required in order to fit the gravity data to our satisfaction.

The final models of both halves of the profile are shown in Figures 1 and 2 and are based on the best fit achieved in both gravity and magnetics. In addition, the models have been checked against drill logs (U.S. Army Corps of Engineers, 1974) where possible, and also against the geologic mapping along the profile (Drewes, 1980). The eastern half has been compared with the NURE magnetic flightlines and the gravity map of the area, as no drill logs were available. Table 1 gives the physical property parameters for all the bodies in the model.

Model Error Estimates

Although the models are the best fit of both the gravity and the magnetic anomaly profiles that we could obtain under the constraints described above, the fit is not perfect and the derived model section is certainly a very simplified approximation of the real subsurface. The modelling program requires that all the prisms in the model be regular in their cross section for the whole length of the body, that each body be homogeneous in its density and magnetic properties, and possess sharp boundaries between properties. None of these conditions are often met in reality, and thus the models are really only aids in visualizing the possible range of actual subsurface configurations. We have used "geological reasonableness" and simplicity to select our final model, even though some other more complex models or models with more extreme physical property values might yield a slightly better fit to some parts of the profile. We feel that the simplest model which fits the potential field data reasonably well yields the most insight into the probable structure and best suggests what steps should be taken to further refine the model.

The western half of the model (Fig.1) is a reasonable fit to the observed gravity and magnetic data, with major misfits only at the 27.5, 39.6, and 43.0 km marks in the magnetic model. These misfits are due to the simplified geometric form of the model. As the first misfit occurs over bedrock, it has no bearing on the basin depth estimate, and can be discounted. The misfit at 39.6 km is due to a man-made object, probably a car, and is also discounted. Finally, the misfit at 43.0 km was found to be impractical to fit with the simplified geometry of the model, although the small anomalies at 39.5-41.0 km and 43.0-45.0 km could be due to bedrock highs not modelled in this study. The gravity model and observed data agree well, with no

misfits of consequence. However, gravity data points from 40.0 km to the end of the profile are sparse and gravity anomalies corresponding to the small magnetic anomalies may be present.

Unfortunately, the eastern half of the profile (Fig. 2) has a worse overall fit in both the gravity and magnetic anomalies. The magnetic model fits well except at the 13.5 km peak and the transition to bedrock. Fitting the 13.5 km peak was also impractical, as it required extremely high magnetic susceptibilities of the dike underneath. The transition to bedrock is also fit poorly due to the very noisy nature of the bedrock and the simplified geometry of the model. To fit the bedrock well would require large numbers of bodies, making the model needlessly complex. As the fit of the first bedrock peak is fairly accurate, the remainder does not have a great effect on the basin magnetic signal, and was left as is. The gravity model of the eastern portion of the profile is adequate, although not exact. Again, making the gravity a better fit entails making the model even more complicated, which was not deemed useful.

Conclusions

The use of both gravity and magnetic anomaly data for the modelling process allows the determination of the interface between the less dense, unconsolidated and the more-dense, consolidated fills in a given basin. Although the assumption of an infinite-depth magnetic basement is unrealistic, the resulting models do give a reasonable basin and interface depth. Further work using more realistic depth approximations for the basement and better initial models based on the geologic mapping is necessary to determine the true power of this method of finding the depth of a basin.

As can be seen in Figure 1, the interface between less-dense (unconsolidated) and more-dense (consolidated) fill varies between very shallow, on the order of a few hundred meters, and relatively thick (approximately 800 meters). The absence of the interface in the eastern portion of Fig. 1 simply reflects the shallower depth to basement of the area. The most easterly portion of Fig. 1, in the vicinity of the San Pedro River and immediately westward (between 29.5 and 32 km) is a very low density fill which becomes the denser top fill of the remainder of the basin as the basin deepens westward. Although the basin deepens considerably at 35.5 km, the less-dense fill actually thins due to the presence of the denser fill underneath. The thickness of this fill in the model may be due to the assumption that the consolidated fill remains a constant density with depth. This simplifies the model and still allows the model to fit the data.

When fitting the magnetic data, it was found that the interface between bodies 7 and 8 (Fig. 1) must be very deep to reproduce the observed magnetic signal. However, the gravity data precluded the possibility of such deep fill. To satisfy both constraints, body 12 was introduced to fill the void left by the magnetic fit. Body 12 is a non-magnetic rock with little density contrast, implying the presence of non- or very weakly magnetic bedrock in that area. The presence of smaller magnetic

anomalies at 39.5-41.0 km and 43.0-45.0 km suggests that perhaps several bodies with possibly shallower depths-to-top may be present in this portion of the basin and more study of this area is merited after more gravity stations are established to better define the anomaly field there. During the magnetic modelling, it was also found to be necessary to introduce a reversely polarized body (Body 2), which would be part of the Cretaceous volcanic rocks of the Tombstone Hills.

The eastern portion of the profile (Fig. 2) has a complicated geometry of basin fill with intercalated volcanic rocks based primarily on nearby geologic mapping (Plate 1). Plate 1 shows there to be a series of volcanic rocks deposited in places on the basement and on a Tertiary conglomerate in others (Drewes, 1980). From the NURE profiles (Plate 3) it was seen that these volcanics were indeed magnetic, and in part reversely polarized. This layer allowed the basin "magnetic" bottom to become extremely shallow in places, as was necessary for fitting the magnetic data. Beneath this volcanic layer in the east is a thin layer of consolidated fill, which is mapped as being under the volcanics elsewhere on the geologic map (Drewes, 1980). There are also three bodies of a dense, non-magnetic bedrock (28, 29, 30, Fig. 2) which were introduced to maintain the magnetic fit while modelling the gravity. Body 17 is the unconsolidated basin fill and bodies 18 and 19 are the consolidated basin fill. The existence of consolidated fill above the volcanic layer in the model implies that either the volcanism was contemporaneous with deposition of the consolidated fill unit or the unconsolidated fill has been densified because of compaction at depth. The two layers serve to model this better than one average layer did.

In both models it should be noted that the probable density of the rhyolitic, and possibly andesitic, rocks of the Cretaceous and Tertiary volcanics may not be all that different from the consolidated fill (for example, the 2.5g/cc density Bronco volcanics and the 2.4 g/cc consolidated fill measured in DH2) and thus the magnetic basement below the consolidated fill could contain a proportion of the volcanic rocks. On the other hand, the parts of the model indicated as consolidated fill are probably not volcanic rocks because the volcanics are magnetic wherever exposed and thus the models would yield a shallower depth estimate than obtained here. In this respect the use of both magnetic and gravity anomaly data yields a model discrimination not available from either dataset alone.

In the west half of the profile, more analysis of the data is merited because of the disagreement of the model with the depth to bedrock at hole DH1 and the fact that the smaller magnetic anomalies in this area were not modelled here. This work awaits more gravity data in the Fort Huachuca Military Reservation area in order to define the gravity anomaly field adequately for more detailed modelling.

References Cited

Brown, S.G., Davidson, E.S., Kister, L.R., Thomsen, B.W., 1966, Water Resources of Fort Huachuca Military Reservation, southeastern Arizona: U.S. Geological

Survey Water-Supply Paper 1819-D, 57p., 2 plates.

Cordell, Lindreth., 1973, Gravity analysis using an exponential density-depth function-San Jacinto Graben, California: *Geophysics*, v 38, no. 4, p.684-690.

Drewes, Harald, 1980, Tectonic map of southeast Arizona: U.S. Geological Survey Miscellaneous Investigations Map I-1109, scale 1:125,000, 2 sheets.

Duska, L., 1958, Maximum gravity effect of certain solids of revolution: *Geophysics* v. 23, p506-519.

Ellett, W.J., 1994, Geologic controls on the occurrence and movement of water in the lower Cienega Creek basin: Dept. of Hydrology and Water Resources MSc. thesis, University of Arizona, 116p.

Gettings, M.E., and Houser, B.B., 1995, Preliminary results of modelling the gravity anomaly field in the southern San Pedro basin, southeastern Arizona: U.S. Geological Survey Open-File Report 95-76, 9p., 5 pl.

Gettings, P.E., Gettings, M.E., and Bultman, M.W., 1995, Data collection and reduction procedures for 1900 km of total intensity magnetic field data collected with a truck-mounted system in southeastern Arizona, southwestern Colorado, and northwestern Wyoming: U.S. Geological Survey Open-File Report 95-32, 13p.

Gilluly, James, 1956, General geology of central Cochise County, Arizona, with sections on age and correlation by A.R. Palmer, J.S. Williams, and J.B. Reeside, Jr.: U.S. Geological Survey Professional Paper 281, 169 p.

Halvorson, P.H.F., 1984, An exploration gravity survey in the San Pedro valley, southeastern Arizona: Dept. of Geosciences MSc. thesis, University of Arizona, 70p., 2 maps.

Hayes, P.T., and Raup, R.B., 1968, Geologic map of the Huachuca and Mustang Mountains, southeastern Arizona: U.S. Geological Survey Miscellaneous Geologic Investigations Map I-509, scale 1:48,000.

Moore, R.B., 1993, Geologic map of the Tombstone Volcanic center, Cochise County, Arizona, U.S. Geological Survey Miscellaneous Investigations Map I-2420, scale 1:50,000, with explanatory text.

Phillips, J.D., Duval, J.S., and Ambroziak, R.A., 1993, National geophysical data grids computer file: gamma-ray, gravity, magnetic, and topographic data for the conterminous United States: U.S. Geological Survey digital data series ; DDS-9, CD-ROM.

Texas Instruments Inc., 1979, Aerial radiometric and magnetic reconnaissance survey of portions of Arizona-New Mexico: U.S. Department of Energy Grand Junction Office Report GJBX-23(79), 7 vols.

Tucci, P., Schmoker, J.W., and Robbins, S.L., 1982, Borehole-gravity surveys in basin-fill deposits of central and southern Arizona: U.S. Geological Survey Open-File Report 82-473, 23p.

U.S. Army Corps of Engineers, Los Angeles District, 1974, Report on water supply, Fort Huachuca and vicinity, Arizona, Appendix 4, Fort Huachuca, Arizona, supplemental report: test well drilling and study of hydrogeologic conditions, Inclosure 5. Geologic logs (16 sheets) and Inclosure 6. Geophysical Logs (12 sheets).

Webring, M., 1985, SAKI: a FORTRAN program for generalized linear inversion of gravity and magnetic profiles: U.S. Geological Survey Open-File Report 85-122, 29p.

Table 1. Density contrast (g/cc), magnetic susceptibility (cgs units), and remnant magnetization vector (cgs intensity), inclination (degrees,+ downward), and declination (degrees, +clockwise off true north) for the model bodies of Figures 1 and 2.

East half of profile (Figure 2)

Body # Density Mag. susc. Rem. int. Rem. incl. Rem. decl.

| Body # | Density | Mag. susc. | Rem. int. | Rem. incl. | Rem. decl. |
|--------|---------|------------|-----------|------------|------------|
| 1 | -0.100 | 4.330E-03 | 0. | 0.0 | 0.0 |
| 2 | 0.000 | 1.106E-03 | 2.500E-03 | -60.0 | 190.0 |
| 3 | 0.000 | 2.000E-03 | 0. | -60.0 | 190.0 |
| 4 | 0.000 | 1.800E-03 | 0. | 0.0 | 0.0 |
| 5 | 0.000 | 6.300E-03 | 0. | 0.0 | 0.0 |
| 6 | 0.000 | 2.974E-03 | 0. | 0.0 | 0.0 |
| 7 | -0.100 | 4.547E-03 | 0. | 0.0 | 0.0 |
| 8 | -0.100 | 7.000E-03 | 0. | 0.0 | 0.0 |
| 9 | -0.100 | 7.124E-03 | 0. | 0.0 | 0.0 |
| 10 | -0.100 | 4.577E-03 | 0. | 0.0 | 0.0 |
| 11 | -0.100 | 5.118E-03 | 0. | 0.0 | 0.0 |
| 12 | -0.100 | 4.000E-03 | 0. | 0.0 | 0.0 |
| 13 | -0.100 | 2.317E-03 | 0. | 0.0 | 0.0 |
| 14 | -0.100 | 3.679E-03 | 0. | 0.0 | 0.0 |
| 15 | -0.100 | 3.775E-03 | 0. | 0.0 | 0.0 |
| 16 | -0.100 | 0. | 0. | 0.0 | 0.0 |
| 17 | -0.604 | 0. | 0. | 0.0 | 0.0 |
| 18 | -0.391 | 0. | 0. | 0.0 | 0.0 |
| 19 | -0.400 | 0. | 0. | 0.0 | 0.0 |
| 20 | -0.160 | 2.800E-03 | 0. | 0.0 | 0.0 |
| 21 | -0.150 | 2.800E-03 | 0. | 0.0 | 0.0 |
| 22 | -0.150 | 7.779E-03 | 0. | 0.0 | 0.0 |
| 23 | -0.150 | 3.930E-03 | 0. | 0.0 | 0.0 |
| 24 | -0.400 | 0. | 0. | 0.0 | 0.0 |
| 25 | 0.000 | 2.000E-03 | 0. | 0.0 | 0.0 |
| 26 | 0.000 | 1.800E-03 | 0. | 0.0 | 0.0 |
| 27 | 0.000 | 2.974E-03 | 0. | 0.0 | 0.0 |
| 28 | 0.000 | 0. | 0. | 0.0 | 0.0 |
| 29 | 0.000 | 0. | 0. | 0.0 | 0.0 |
| 30 | 0.000 | 0. | 0. | 0.0 | 0.0 |

Table 1. (cont'd.)

West half of profile (Figure 1)

Body # Density Mag. susc. Rem. int. Rem. incl. Rem. decl.

| | | | | | |
|----|--------|-----------|-----------|-------|-------|
| 1 | 0.024 | 7.209E-04 | 0. | 0.0 | 0.0 |
| 2 | -0.009 | 6.207E-04 | 1.300E-03 | -60.0 | 190.0 |
| 3 | -0.004 | 5.618E-03 | 0. | 0.0 | 0.0 |
| 4 | 0.010 | 7.670E-03 | 0. | 0.0 | 0.0 |
| 5 | 0.060 | 4.462E-03 | 0. | 0.0 | 0.0 |
| 6 | 0.068 | 2.425E-03 | 0. | 0.0 | 0.0 |
| 7 | -0.035 | 6.597E-03 | 0. | 0.0 | 0.0 |
| 8 | -0.020 | 1.363E-03 | 0. | 0.0 | 0.0 |
| 9 | -0.020 | 1.150E-03 | 0. | 0.0 | 0.0 |
| 10 | 0.025 | 5.686E-03 | 0. | 0.0 | 0.0 |
| 11 | -0.602 | 0. | 0. | 0.0 | 0.0 |
| 12 | -0.082 | 0. | 0. | 0.0 | 0.0 |
| 13 | -0.422 | 0. | 0. | 0.0 | 0.0 |
| 14 | -0.644 | 0. | 0. | 0.0 | 0.0 |

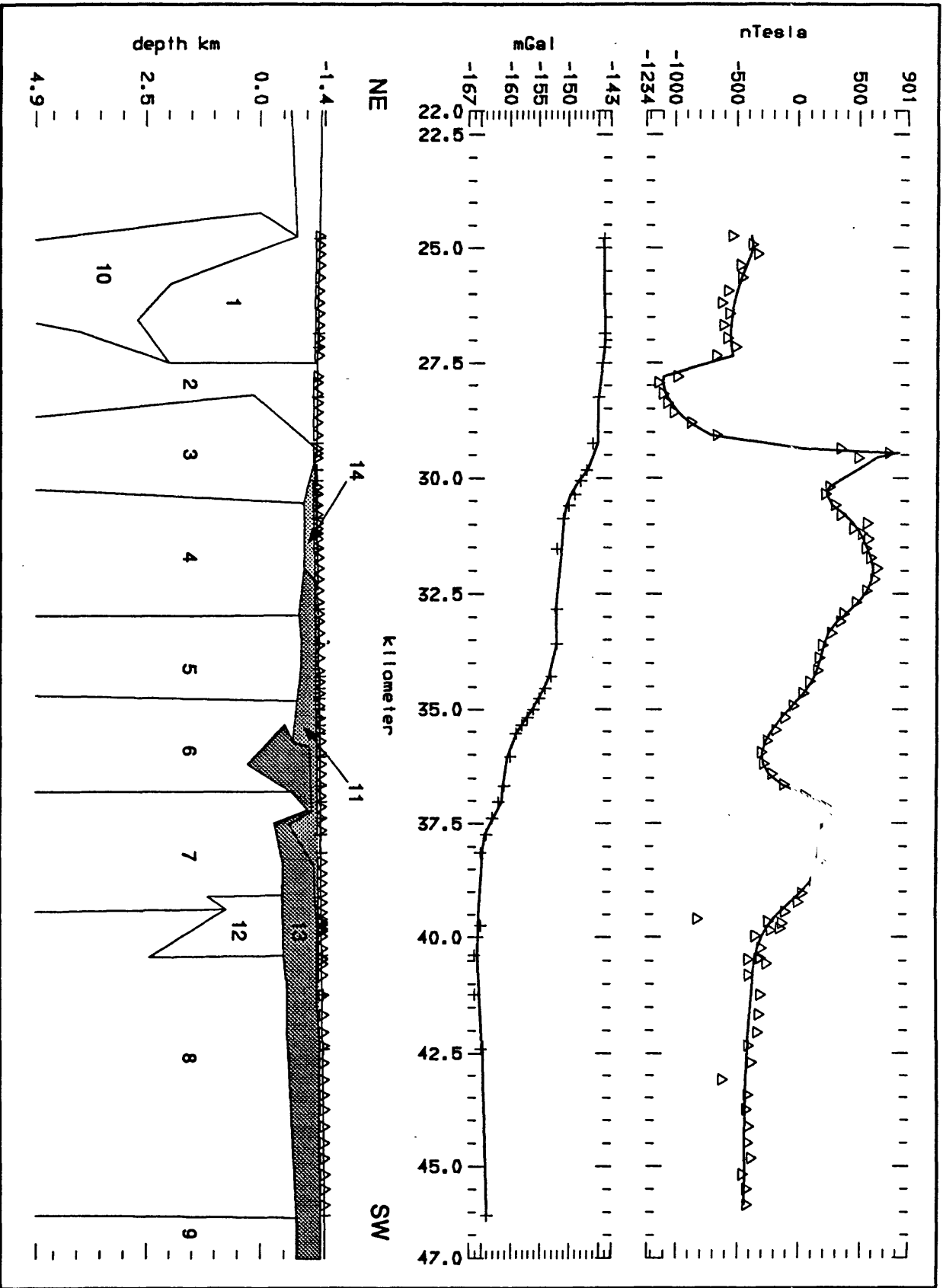


Figure 1. Western portion of profile (viewed from the northwest so northeast is to the left and southwest is to the right), showing the San Pedro basin area. The San Pedro River is at about kilometer 30.0. Basin fill is bodies 11 and 14 (unconsolidated) and body 13 (consolidated). All other bodies are basement; body 12 is non-magnetic basement.

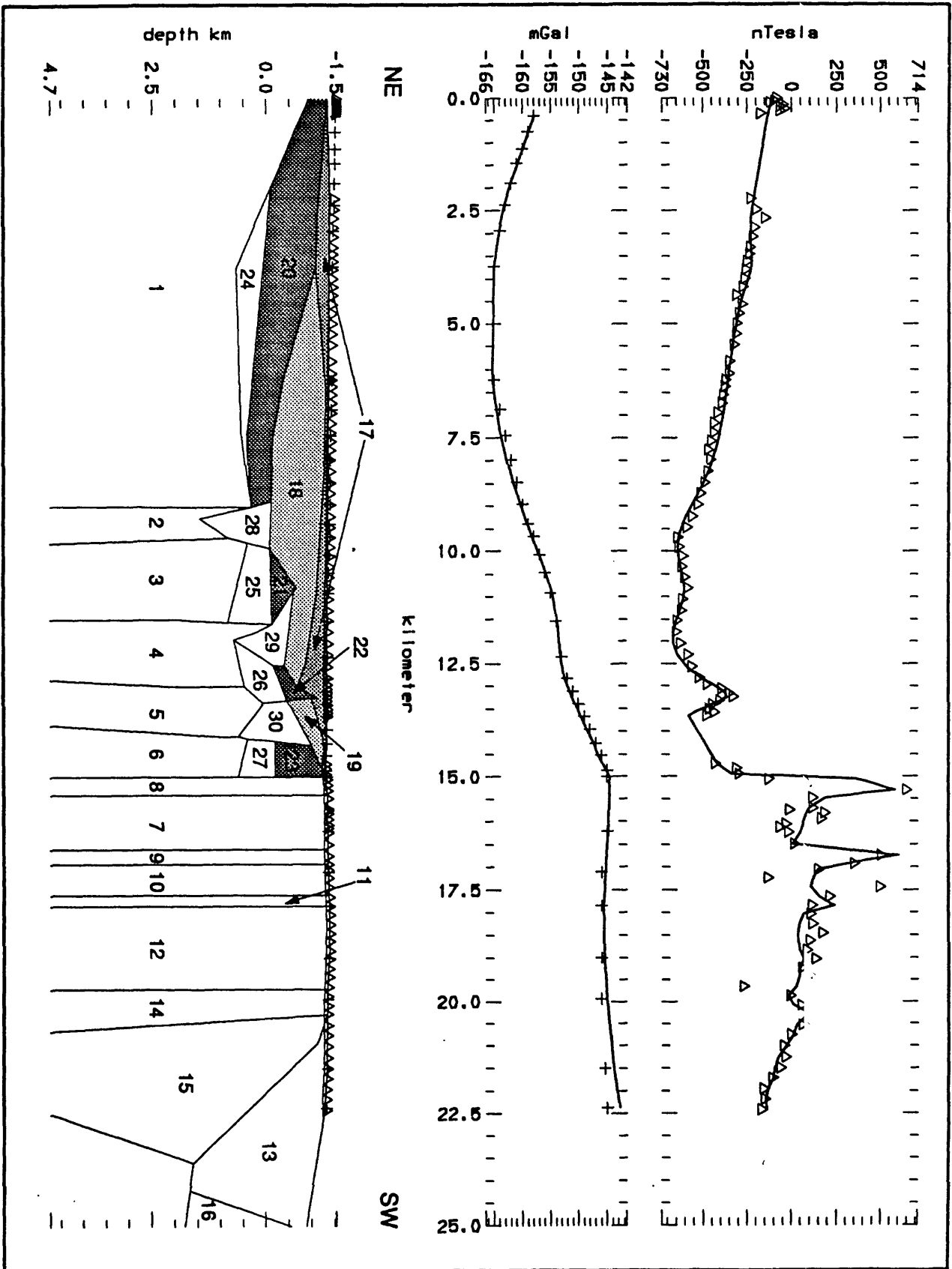


Figure 2. Eastern portion of profile, showing Tombstone basin. Bodies 17, 18, and 19 indicate the basin fill. Body 17 is the unconsolidated portion of the fill. Bodies 20 to 23 are the volcanic layer, and body 24 is the lower conglomerate. Bodies 28, 29, and 30 are non-magnetic basement. All others are basement, including highly susceptible dikes (bodies 5, 8, 9, and 11). Profile is viewed looking southeast so northeast is to the left, southwest is to the right.